



Can Cosmological Simulations Reproduce the Spectroscopically Confirmed Galaxies Seen at $z \geq 10$?

B. W. Keller¹, F. Munshi², M. Trebitsch³, and M. Tremmel⁴¹ Department of Physics and Materials Science, University of Memphis, 3720 Alumni Avenue, Memphis, TN 38152, USA; bkeller1@memphis.edu² Department of Physics and Astronomy, George Mason University, 4400 University Drive, MSN 3F3, Fairfax, VA 22030-4444, USA³ Kapteyn Astronomical Institute, University of Groningen, P.O. Box 800, 9700 AV Groningen, The Netherlands⁴ Physics Department, University College Cork, Cork T12 K8AF, Ireland

Received 2022 December 24; accepted 2023 January 6; published 2023 February 6

Abstract

Recent photometric detections of extreme ($z > 10$) redshift galaxies from the JWST have been shown to be in strong tension with existing simulation models for galaxy formation and in the most acute case, in tension with Λ CDM itself. These results, however, all rest on the confirmation of these distances by spectroscopy. Recently, the JADES survey has detected the most distant galaxies with spectroscopically confirmed redshifts, with four galaxies found with redshifts between $z = 10.38$ and $z = 13.2$. In this Letter, we compare simulation predictions from four large cosmological volumes and two zoom-in protoclusters with the JADES observations to determine whether these spectroscopically confirmed galaxy detections are in tension with existing models for galaxy formation or with Λ CDM more broadly. We find that existing models for cosmological galaxy formation can generally reproduce the observations for JADES in terms of galaxy stellar masses, star formation rates, and the number density of galaxies at $z > 10$.

Unified Astronomy Thesaurus concepts: [Astronomical simulations \(1857\)](#); [Hydrodynamical simulations \(767\)](#); [Cosmology \(343\)](#); [Galaxy formation \(595\)](#); [Protogalaxies \(1298\)](#)

1 Introduction

The successful deployment of the JWST has already produced observations of the highest-redshift galaxies detected to date. The first sets of detections reported (Naidu et al. 2022a; Finkelstein et al. 2022; Labbe et al. 2022; Adams et al. 2023) have found galaxies with $M_* > 10^8 M_\odot$ at $z_{\text{phot}} > 10$. The most extreme of these examples, with $M_* > 10^{10} M_\odot$ at $z_{\text{phot}} > 10$ have already been shown to be in strong tension with Λ CDM (Boylan-Kolchin 2022; Haslbauer et al. 2022). These tensions have, however, been clouded by the large uncertainty in fitting photometric redshifts at such extreme distances (Naidu et al. 2022b; Bouwens et al. 2022; Kaasinen et al. 2022). Naidu et al. (2022b) and Zavala et al. (2022) found that breaks in the spectral energy distribution (SED) produced by dust obscuration at $z \sim 5$ can masquerade as a Lyman break at $z \sim 17$ for recent JWST observations (see also Fujimoto et al. 2022 for a similar effect in Atacama Large Millimeter/submillimeter Array, ALMA, observations).

As Boylan-Kolchin (2022) showed, if the comoving number density of galaxies at $z = 10$ with $M_* > 10^{10} M_\odot$ is as high as can be estimated from Labbe et al. (2022), it would be a significant challenge for Λ CDM, analogous to Haldane’s “fossil rabbits in the Precambrian” (Harvey et al. 1996). Haslbauer et al. (2022) have shown that the observations of galaxies with high stellar mass ($M_* > 10^9$) at high redshift $z \gtrsim 10$ from Adams et al. (2023), Labbe et al. (2022), Naidu et al. (2022a), and Naidu et al. (2022b) are in extreme tension with the simulation predictions of EAGLE (Schaye et al. 2015), TNG50, and TNG100 (Pillepich et al. 2018a; Nelson et al. 2019a). These authors warn, however, that spectroscopic

confirmation of redshifts is needed before final conclusions can be reached: these tensions all rest on the estimations of stellar masses provided by SED fitting and critically, on the distance estimates themselves. Without spectroscopic confirmation of the redshifts reported in these observations, these potential tensions may be illusory: artifacts of overestimated distances and thus overestimated intrinsic luminosities. Indeed, as Behroozi et al. (2020) have shown, semiempirical modeling of galaxy formation in Λ CDM predicts JWST-detectable galaxies with $M_* > 10^7 M_\odot$ to at least $z \sim 13.5$.

Spectroscopic confirmation has now arrived with the discovery in the JADES survey of four galaxies with $z_{\text{spec}} > 10$ and $M_* \gtrsim 10^8 M_\odot$ (Curtis-Lake et al. 2022; Robertson et al. 2022). By observing 65 arcmin² of the GOODS-S field with JWST NIRCcam and NIRSpec, JADES has confirmed the four earliest detected galaxies: JADES-GS-z10-0 at $z = 10.38_{-0.06}^{+0.07}$, JADES-GS-z11-0 at $z = 11.58_{-0.05}^{+0.05}$, JADES-GS-z12-0 at $z = 12.63_{-0.08}^{+0.24}$, and JADES-GS-z13-0 at $z = 13.2_{-0.07}^{+0.04}$. Curtis-Lake et al. (2022) and Robertson et al. (2022) have measured stellar masses and star formation rates (SFRs) for these galaxies using the Prospector SED-fitting code (Johnson et al. 2021), finding them to be compact, star-forming galaxies with young stellar populations and relatively high star formation surface densities.

In this Letter, we compare the observed JADES galaxies to predictions from an array of large cosmological hydrodynamical simulations. These simulations reproduce observed galaxy population statistics (such as the observed galaxy stellar mass function and fundamental plane of star formation) at low redshift. With JADES, we are able to test whether those same models for galaxy formation fail to reproduce these new observations of high-redshift galaxy formation.

2 Simulation Data

In order to probe the predictions of current galaxy formation models, we examine simulation data from EAGLE (Crain et al.

Table 1
Simulation Data Compared in This Study

Simulation	Cosmology	Box Size (cMpc)	z Range	N_{snap}	$M_{\text{DM}} (M_{\odot})$	$M_{\text{baryon}} (M_{\odot})$
EAGLE	Planck 2013 (Planck Collaboration et al. 2014)	100	9.99	1	9.7×10^6	1.81×10^6
Illustris	WMAP-9 (Hinshaw et al. 2013)	106.5	10.00–13.34	7	6.3×10^6	1.3×10^6
TNG100	Planck 2015 (Planck Collaboration et al. 2016)	110.7	10.00–11.98	3	7.5×10^6	1.4×10^6
Simba	Planck 2015 (Planck Collaboration et al. 2016)	147.7	9.96–13.70	10	9.7×10^7	1.82×10^7
OBELISK	WMAP-7 (Komatsu et al. 2011)	142.0 ^a	10.07–13.77	13	1.2×10^6	1×10^4
RomulusC	Planck 2015 (Planck Collaboration et al. 2016)	50 ^a	9.97–12.88	2	3.4×10^5	2.1×10^5

Note. Each cosmological volume has a box of side length ~ 100 cMpc. We show the choice of cosmological parameters, box size, redshift range between $z \sim 10$ –14, number of snapshot outputs in that range, and resolution for DM and baryons. OBELISK is an Eulerian simulation, and thus the baryonic resolution reported here is given as the typical mass of a star particle and the mass of a gas cell with $\Delta x = 35$ pc at a density of $n > 10 \text{ cm}^{-3}$.

^a Zoom-in simulation of an individual galaxy protocluster, drawn from a lower-resolution volume.

2015; Schaye et al. 2015; McAlpine et al. 2016), Illustris (Vogelsberger et al. 2014a, 2014b; Genel et al. 2014; Nelson et al. 2015), TNG100 (Pillepich et al. 2018b; Marinacci et al. 2018; Naiman et al. 2018; Nelson et al. 2018; Springel et al. 2018; Nelson et al. 2019b), and Simba (Davé et al. 2019) cosmological volumes. Each of these simulations has a volume of $\sim 10^6 \text{ cMpc}^3$, with baryonic mass resolution of $10^6 M_{\odot}$ – $10^7 M_{\odot}$, which allows them to (marginally) resolve the formation of $M_* = 10^8 M_{\odot}$ – $10^9 M_{\odot}$ galaxies (an $M_* = 5 \times 10^8 M_{\odot}$ galaxy in EAGLE, Illustris, TNG100, and Simba will contain 276, 384, 357, and 27 star particles respectively). Each of these projects includes models for gas cooling, star formation, and feedback from supernovae (SNe) and active galactic nuclei (AGNs) that are tuned to reproduce the $z \sim 0$ stellar mass function (among other low-redshift population statistics). In Table 1 we list the cosmological parameters used for each simulation, as well as the size of the simulation volume, the range and number of snapshots with redshift between $z \sim 10$ and $z \sim 14$, and the mass resolution for dark matter (DM) and baryonic particles. We rely on the public releases of the halo catalogs from each simulation to determine galaxy stellar masses and SFRs in these simulation data sets.

We have also included data from the cosmological zoom-in simulations OBELISK (Trebitsch et al. 2021) and RomulusC (Tremmel et al. 2019). OBELISK is a zoom-in of the most massive halo at $z=2$ in the HORIZON-AGN volume (Dubois et al. 2014). This region is selected to include all DM particles within $4R_{\text{vir}}$ of the halo center at $z=2$. At $z=0$, this cluster has a halo mass of $M_{\text{halo}} \sim 6.6 \times 10^{14} M_{\odot}$. RomulusC is a zoom-in simulation of a smaller galaxy cluster, with halo mass $M_{\text{halo}} = 1.5 \times 10^{14} M_{\odot}$ at $z=0$. It is drawn from a 50^3 cMpc^3 DM-only volume and applies the same modeling approach for cooling, star formation, supermassive black hole (SMBH) evolution, and feedback as the Romulus volume (Tremmel et al. 2017). Unlike the other data sets we examine here, these zooms do not include a full resolution sample of a large volume; instead they offer a higher-resolution picture of early collapsing overdensities.

3 Results

We begin by simply showing the distribution of galaxy stellar masses in each simulation volume as a function of redshift, shown in Figure 1. Not all of the simulations we examine here have well-sampled snapshots above $z=10$ (EAGLE in particular only includes one snapshot between $z \sim 10$ and $z \sim 14$). However, as can be seen, all of the

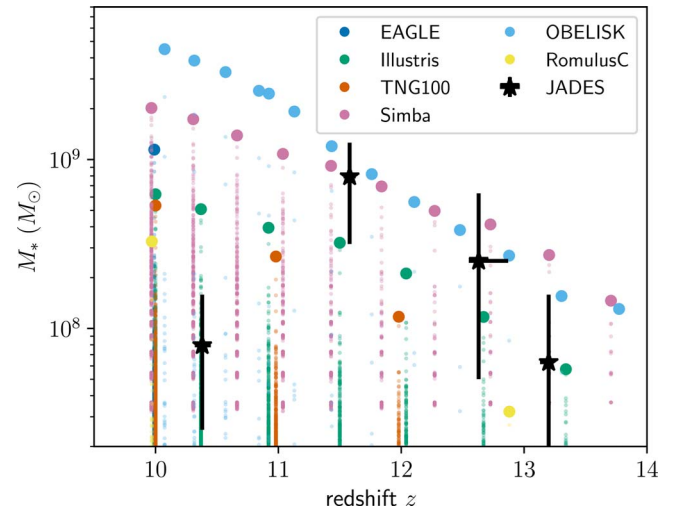


Figure 1. Stellar mass of galaxies from various simulation volumes as a function of redshift. Black stars with error bars show the Robertson et al. (2022) JADES observations, while colored points show individual galaxies from different simulated volumes. Large colored points show the most massive galaxy at each redshift for a given simulation.

simulations produce a large number of galaxies with $M_* > 10^8 M_{\odot}$ at $z \sim 10$. At all redshifts, Simba and OBELISK produce the most massive galaxies of the simulations we examine, in part due to the larger volume they simulate/are drawn from (~ 2.4 times the comoving volume of TNG100, the next largest volume), as well as differences in the choice of subgrid physics models. As we move to higher redshift, only Simba and OBELISK produce even a single galaxy above the best-fit stellar masses of JADES-GS-z11-0, JADES-GS-z12-0, and JADES-GS-z13-0. Illustris and TNG100 are unable to produce galaxies at $z \sim 11.5$ –12 that reach even the lower estimate for the stellar mass of JADES-GS-z11-0.

As Robertson et al. (2022) has also provided estimates for the SFRs in the 4 JADES observations, we show in Figure 2 the SFR- M_* plane for simulated galaxies at $z \sim 10$. All simulation volumes produce galaxies at $z \sim 10$ with specific star formation rates (sSFR) = 10 Gyr^{-1} , except for RomulusC, which has an sSFR roughly half this value. An sSFR of 10 Gyr^{-1} is approximately 4 times higher than the star-forming main sequence at $z=2$ (Rodighiero et al. 2011), consistent with the observed trend of increasing sSFR toward higher $z \sim 6$ redshift (Santini et al. 2017). The banding seen in the lower-mass Simba galaxies is simply a function of resolution, as these galaxies contain only a handful of star particles. Interestingly,

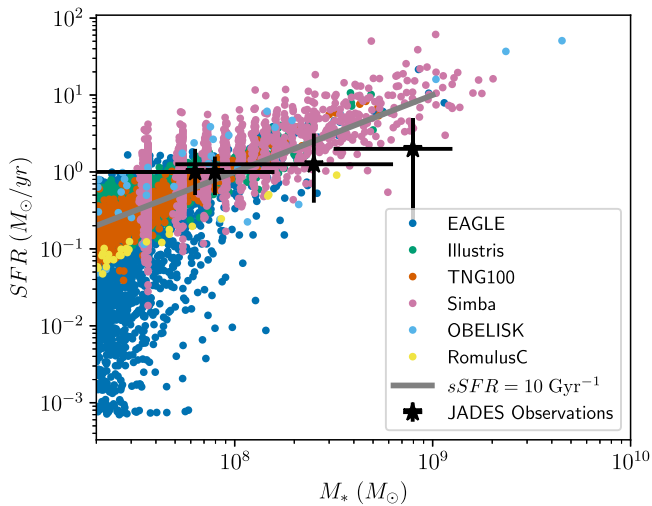


Figure 2. SFR vs. stellar mass for simulated galaxies at $z \sim 10$ and observed galaxies at $z \geq 10$. Simulation data are shown as colored points, while the JADES observations are shown as black stars. A constant $sSFR$ of 10 Gyr^{-1} is shown with the gray line.

there appears to be no noticeable trend in the SFR as a function of stellar mass for the JADES observations. However, drawing strong conclusions as to the nature of the SFR– M_* relation at $z \geq 10$ is ill advised given the small number of observations, their relatively large uncertainties, and the intrinsic scatter in the SFR– M_* plane that the simulations predict. Beyond these, the NIRSpc observations of the JADES galaxies are selected from photometric observations, which are subject to a continuum flux (and therefore SFR) limit, introducing a potential observational bias. Overall, the SFRs measured from the simulations match the JADES observations reasonably well though with perhaps higher SFRs for simulated galaxies at masses above $M_* \sim 5 \times 10^8 M_\odot$. Further observations will help reveal if the flat SFR– M_* curve is a real feature of $z \geq 10$ galaxy formation or simply an artifact of the small sample size of the spectroscopically confirmed JADES galaxies and/or uncertainties in the estimation of M_* or SFR.

In order to make a more quantitative estimate of potential tension between simulated cosmological volumes and the Robertson et al. (2022) observations, we now look to the comoving number density of galaxies at each of the redshifts probed by JADES. The deep observing area of JADES, using the JWST NIRCam, (9.7 arcmin^2), yields a volume of $V \sim (9 \times 9 \times 494) \text{ cMpc}^3 \sim 4 \times 10^4 \text{ cMpc}^3$ bounded by the comoving distance of 494 Mpc between the JADES-GS-z10-0 at $z = 10.38$ and JADES-GS-z13-0 at $z = 13.2$. These candidates were, however, originally selected photometrically from a wider field of 65 arcmin^2 , which yields a volume of $V \sim 2.7 \times 10^5 \text{ cMpc}^3$. We can thus estimate the number density of the JADES galaxy observations as $n \sim 3.7 \times 10^{-6} \text{ cMpc}^{-3}$. In Figure 3, we show the comoving number density of galaxies above a given stellar mass for simulation snapshots nearest in redshift to each of the JADES observations (if the nearest snapshot is separated by more than 0.5 in redshift, we omit it from the plot). Each of the JADES observations above $z > 10.38$ implies a slightly higher number density than what is produced by the simulations. We also show the estimated number density assuming a constant stellar baryon conversion efficiency ($M_* = \epsilon f_B M_{\text{halo}}$) of $\epsilon = 0.1$ and the maximum expected number density (with $M_* = f_B M_{\text{halo}}$), following

Boylan-Kolchin (2022) using a Sheth & Tormen (1999) halo mass function. Each of the JADES galaxies lies outside of the excluded region of $M_* = f_B M_{\text{halo}}$, but the most extreme two cases (JADES-GS-z11-0 and JADES-GS-z12-0) imply integrated baryon conversion efficiencies near 10% ($M_*/(f_B M_{\text{halo}}) \sim 0.1$). For $z \sim 10$, we also show the independent measurements for the galaxy stellar mass function measured by the GREATS ALMA survey by Stefanon et al. (2021). The highest-predicted number density for massive halos at these redshifts is from Simba, and only JADES-GS-z11-0 and JADES-GS-z12-0 imply number densities higher than in Simba for galaxies at their stellar mass. Even for the most extreme case, JADES-GS-z11-0, the probability of finding a galaxy with stellar mass above $M_* = 10^{8.9} M_\odot$ at $z \sim 11$, in a random volume of $2.7 \times 10^5 \text{ cMpc}^3$ in Simba, is 8%. If we instead take the lower estimate for the stellar masses from JADES-GS-z11-0 ($M_* = 10^{8.5} M_\odot$), this probability rises to 92%. There does not appear to be any significant tension in the density of galaxies with $M_* \sim 10^8 M_\odot$ at $z > 10$ inferred from JADES and the number density produced by at least one existing cosmological simulation (Simba).

4 Discussion

We have compared the recent detection of spectroscopically confirmed $z > 10$ galaxies from the JADES survey to the EAGLE, Illustris, TNG100, and Simba surveys. We show that all four simulation suites produce galaxies with $M_* \sim 10^{8.5} M_\odot$ at $z \sim 10$ and that Simba in particular produces at least one galaxy with mass comparable to the JADES observations at each observed redshift. The JADES galaxies show a relatively flat SFR– M_* trend, in contrast to the constant $sSFR$ of ~ 5 – 10 Gyr^{-1} for simulated galaxies at $z \sim 10$. Comparing the estimated JADES galaxy stellar mass functions to the simulation predictions shows that these simulations are in reasonable agreement with the number density of galaxies at $z \sim 10$ observed by JADES and the earlier ALMA measurements from Stefanon et al. (2021; though Illustris and TNG100 appear to be slightly underpredicting the formation of galaxies at $z \sim 10$). At $z \sim 11$ – 12 , JADES implies a slightly higher number density of galaxies at $M > 10^8 M_\odot$ than are predicted by any of the simulation volumes we examine here. We find, however, that given the small number of objects confirmed in JADES (in a volume of $\sim 2.7 \times 10^5 \text{ cMpc}^3$), none of the JADES observations is in greater than 2σ tension for the best-fit stellar mass, relative to the Simba simulation. JADES-GS-z11-0 implies a slightly higher density at $z = 11$ for galaxies with $M_* \sim 10^9 M_\odot$, but the difference between Simba and density inferred from JADES is only slight. A randomly chosen volume of $2.7 \times 10^5 \text{ cMpc}^3$ from Simba at $z = 11.4$ will contain a galaxy with stellar mass greater than that of JADES-GS-z11-0 8% of the time. At the lower uncertainty for the JADES-GS-z11-0 stellar mass, this probability grows to 92%.

As future observations better constrain the stellar mass function at $z \sim 11$, this tension may strengthen or disappear. If objects as massive as those seen by Labbe et al. (2022), Adams et al. (2023), and Naidu et al. (2022a) are confirmed to be common, with spectroscopic redshifts of $z > 10$, this would imply a serious problem with existing Λ CDM and galaxy formation theory (Boylan-Kolchin 2022; Haslbauer et al. 2022; Lovell et al. 2023). In order to be in tension with all models for galaxy formation in Λ CDM (by implying galaxy star formation

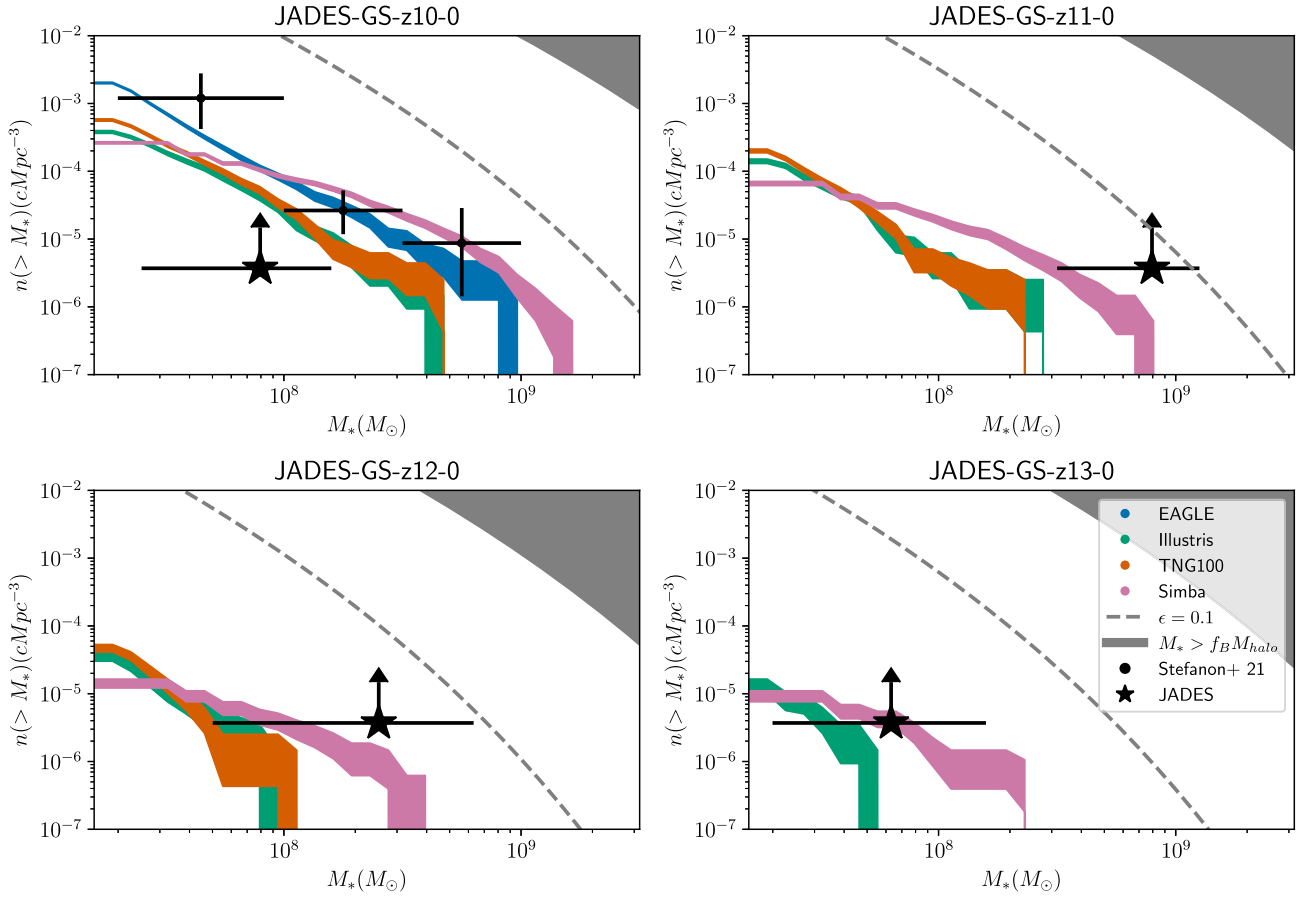


Figure 3. Cumulative number density of galaxies above a given stellar mass for simulation snapshots (colored areas) at the nearest redshift to the JADES observations. Snapshots are chosen such that no more than $\Delta z = 0.5$ separates the simulation snapshot redshift from the observed redshift. Black stars show the detections from Robertson et al. (2022). Filled colored areas show the uncertainty from Poisson sampling of each mass bin. The gray dashed curve shows the expected number density for an integrated star formation efficiency ϵ of 10%, and the shaded gray area shows the excluded region where more stellar mass is produced in halos than their available baryon budget. Black circles at $z \sim 10$ show the estimated number density from observations by Stefanon et al. (2021). We exclude from this figure the data from zoom-in simulations.

efficiencies $>100\%$), the number density of $M_* = 10^9 M_\odot$ galaxies at $z \sim 11$ would need to be more than 3 orders of magnitude higher than what is implied by the JADES-GS-z11-0 detection. This tension may be resolved by future refinements in the SED-fit stellar mass estimates lowering the stellar mass measured for JADES-GS-z11-0 or simply by JADES-GS-z11-0 residing in a moderately rare ($P \sim 8\%$) overdensity. For a mean cosmological mass density of $\rho_m \sim 4 \times 10^{10} M_\odot \text{cMpc}^{-3}$, a comoving volume of $4 \times 10^4 \text{cMpc}^3$ contains a total mass of $\sim 10^{15} M_\odot$. If the entire volume covered by the deepest JADES observations is a rare overdensity that will eventually collapse to form a $z \sim 0$ cluster, it will be on the order of the most massive clusters detected (Lovell et al. 2023). It is unlikely that the entire JADES volume is probing a single large overdensity (given the fact that it is a pencil-beam volume with a comoving depth of 494cMpc over an area on the sky of only $(9 \times 9) \text{cMpc}^2$), but the possibility that one or more of the JADES galaxies above $z > 10$ resides within one or more protoclusters such as those simulated in OBELISK is still plausible.

One question that arises from this data is why the Simba simulations predict more $M_* > 10^8 M_\odot$ galaxies at $z > 10$ than Illustris and TNG100. While the Simba volume is somewhat larger than Illustris and TNG100 (Simba’s volume is ~ 2.4 times larger than TNG100), it also produces a higher density of

galaxies with $M_* > 10^8 M_\odot$ at all redshifts we have examined here. Each of these simulations applies a different set of models for star formation and feedback by SNe and AGNs. In Simba, SMBHs are seeded in galaxies with $M_* > 10^{9.5} M_\odot$, while in TNG100 SMBHs are seeded in halos with $M_{\text{halo}} > 7.4 \times 10^{10} M_\odot$. This means that none of the galaxies we show in Figure 1 or in Figure 3 contain SMBHs, so the differences we find must be a function of the different star formation and feedback recipes used in TNG100 and Simba. Simba applies a tuned reduction in the SN-driven outflow mass loadings η above $z > 3$ to better match observations of the galaxy stellar mass function at $z > 6$, lowering the mass loadings by $(a/0.25)^2$ (Davé et al. 2019). It appears that lower-mass loadings at high redshift are not only important to matching observations at $z \sim 6$ but for $z > 10$ as well. Understanding how SNe regulate galaxy formation and drive outflows in these early epochs will be an important avenue of future simulation study.

While the results we have shown here show that there is no strong tension between at least one existing large-volume cosmological simulation and the spectroscopically confirmed galaxy detections from JADES, it is important to note that the cosmological volumes we have examined here are all relatively low resolution: even a $10^9 M_\odot$ galaxy only contains ~ 50 star particles in Simba. These simulations are also tuned to reproduce $z \sim 0$ galaxy properties. Star formation and feedback

at low redshift are still relatively poorly understood processes (Naab & Ostriker 2017), a problem that becomes much more severe at epochs as early as $z > 10$ (Visbal et al. 2020).

An obvious direction for future studies is to search for galaxies of similar mass in higher-resolution, high-redshift simulation volumes. In particular, simulations designed to study reionization, such as Renaissance (O’Shea et al. 2015), OBELISK (Trebitsch et al. 2021), and SPHINX (Rosdahl et al. 2018), all achieve resolutions significantly higher than any of the volumes we have studied here. Many also feature more physically motivated models for stellar feedback, which are possible at these higher resolutions. Even at the same resolution as these ($\sim 100 \text{ Mpc}^3$) volumes, rare regions can be probed by zooming in on overdensities from much larger volumes, a strategy applied by FLARES (Lovell et al. 2021). FLARES produces a stellar mass function at $z \sim 10$ consistent with Stefanon et al. (2021), which we show here to be consistent with JADES. Zoom-in simulations of protoclusters such as OBELISK will be particularly fruitful, as the earliest bright galaxies to form are likely to be found in these environments. As we show in Figure 1, OBELISK contains a number of simulated galaxies with comparable stellar masses to each of the JADES detections at every redshift of the JADES sample, resolved with > 1000 star particles. Zoom-in simulations such as these will be a powerful tool for understanding the earliest phase of galaxy formation at $z > 10$.

5 Conclusions

We have compared the recent observations of the highest-redshift galaxies with spectroscopically confirmed distances from the JADES survey (Robertson et al. 2022) to simulated galaxies from EAGLE, Illustris, TNG100, and Simba volumes and the OBELISK and RomulusC zoom-ins. In general, we find that each of these simulations produces galaxies with comparable stellar masses to the JADES galaxies by $z \sim 10$. The most massive JADES galaxies have somewhat lower SFRs than simulated galaxies at $z \sim 10$ but lie within the scatter of the simulations. The galaxy number density implied by the JADES galaxies at $z \sim 10$ is consistent with both the simulations and past observations. At higher redshift, only Simba and OBELISK produce galaxies as massive as those found in JADES. The number density of galaxies inferred from JADES is slightly larger than what is predicted by Simba at $z = 11$ and $z = 12$ but at a low level of significance. Overall, there appears to be no strong tension between models for galaxy formation in cosmological hydrodynamic simulations and the most distant spectroscopically confirmed galaxies.

B.W.K would like to thank Tessa Klotzl for incredible support and help editing this manuscript. M.Trebitsch acknowledges support from the NWO grant 0.16.VIDI.189.162 (“ODIN”). We also would like to thank James Wadsley for useful discussions and Jordan Van Nest in helping with the RomulusC simulation data. We especially would like to thank the teams behind EAGLE, Illustris, TNG, and Simba for providing public access to their simulation data sets. This study would have been impossible to complete in a timely fashion without the community spirit behind these public releases.

We acknowledge the Virgo Consortium for making their simulation data available. The EAGLE simulations were performed using the DiRAC-2 facility at Durham, managed

by the ICC, and the PRACE facility Curie based in France at TGCC, CEA, Bruyères-le-Châtel.

The IllustrisTNG simulations were undertaken with compute time awarded by the Gauss Centre for Supercomputing (GCS) under GCS Large-Scale Projects GCS-ILLU and GCS-DWAR on the GCS share of the supercomputer Hazel Hen at the High Performance Computing Center Stuttgart (HLRS), as well as on the machines of the Max Planck Computing and Data Facility (MPCDF) in Garching, Germany.

ORCID iDs

B. W. Keller  <https://orcid.org/0000-0002-9642-7193>

F. Munshi  <https://orcid.org/0000-0002-9581-0297>

M. Trebitsch  <https://orcid.org/0000-0002-6849-5375>

M. Tremmel  <https://orcid.org/0000-0002-4353-0306>

References

- Adams, N. J., Conselice, C. J., Ferreira, L., et al. 2023, *MNRAS*, 518, 4755
- Behroozi, P., Conroy, C., Wechsler, R. H., et al. 2020, *MNRAS*, 499, 5702
- Bouwens, R., Illingworth, G., Oesch, P., et al. 2022, arXiv:2212.06683
- Boylan-Kolchin, M. 2022, arXiv:2208.01611
- Crain, R. A., Schaye, J., Bower, R. G., et al. 2015, *MNRAS*, 450, 1937
- Curtis-Lake, E., Carniani, S., Cameron, A., et al. 2022, arXiv:2212.04568
- Davé, R., Anglés-Alcázar, D., Narayanan, D., et al. 2019, *MNRAS*, 486, 2827
- Dubois, Y., Pichon, C., Welker, C., et al. 2014, *MNRAS*, 444, 1453
- Finkelstein, S. L., Bagley, M. B., Ferguson, H. C., et al. 2022, arXiv:2211.05792
- Fujimoto, S., Finkelstein, S. L., Burgarella, D., et al. 2022, arXiv:2211.03896
- Genel, S., Vogelsberger, M., Springel, V., et al. 2014, *MNRAS*, 445, 175
- Harvey, P., Meeting, R. S. G. B. D., Brown, A., & Smith, J. 1996, *New Uses for New Phylogenies* (Oxford: Oxford Univ. Press)
- Haslbauer, M., Kroupa, P., Zonoozi, A. H., & Hagh, H. 2022, *ApJL*, 939, L31
- Hinshaw, G., Larson, D., Komatsu, E., et al. 2013, *ApJS*, 208, 19
- Johnson, B. D., Leja, J., Conroy, C., & Speagle, J. S. 2021, *ApJS*, 254, 22
- Kaasinen, M., van Marrewijk, J., Popping, G., et al. 2022, arXiv:2210.03754
- Komatsu, E., Smith, K. M., Dunkley, J., et al. 2011, *ApJS*, 192, 18
- Labbe, I., van Dokkum, P., Nelson, E., et al. 2022, arXiv:2207.12446
- Lovell, C. C., Harrison, I., Harikane, Y., Tacchella, S., & Wilkins, S. M. 2023, *MNRAS*, 518, 2511
- Lovell, C. C., Vijayan, A. P., Thomas, P. A., et al. 2021, *MNRAS*, 500, 2127
- Marinacci, F., Vogelsberger, M., Pakmor, R., et al. 2018, *MNRAS*, 480, 5113
- McAlpine, S., Helly, J. C., Schaller, M., et al. 2016, *A&C*, 15, 72
- Naab, T., & Ostriker, J. P. 2017, *ARA&A*, 55, 59
- Naidu, R. P., Oesch, P. A., & Dokkum, P. v. 2022a, *ApJL*, 940, L14
- Naidu, R. P., Oesch, P. A., Setton, D. J., et al. 2022b, arXiv:2208.02794
- Naiman, J. P., Pillepich, A., Springel, V., et al. 2018, *MNRAS*, 477, 1206
- Nelson, D., Pillepich, A., Genel, S., et al. 2015, *A&C*, 13, 12
- Nelson, D., Pillepich, A., Springel, V., et al. 2018, *MNRAS*, 475, 624
- Nelson, D., Pillepich, A., Springel, V., et al. 2019a, *MNRAS*, 490, 3234
- Nelson, D., Springel, V., Pillepich, A., et al. 2019b, *ComAC*, 6, 2
- O’Shea, B. W., Wise, J. H., Xu, H., & Norman, M. L. 2015, *ApJL*, 807, L12
- Pillepich, A., Springel, V., Nelson, D., et al. 2018a, *MNRAS*, 473, 4077
- Pillepich, A., Nelson, D., Hernquist, L., et al. 2018b, *MNRAS*, 475, 648
- Planck Collaboration, Ade, P. A. R., Aghanim, N., et al. 2014, *A&A*, 571, A16
- Planck Collaboration, Ade, P. A. R., Aghanim, N., et al. 2016, *A&A*, 594, A13
- Robertson, B. E., Tacchella, S., Johnson, B. D., et al. 2022, arXiv:2212.04480
- Rodighiero, G., Daddi, E., Baronchelli, I., et al. 2011, *ApJL*, 739, L40
- Rosdahl, J., Katz, H., Blaizot, J., et al. 2018, *MNRAS*, 479, 994
- Santini, P., Fontana, A., Castellano, M., et al. 2017, *ApJ*, 847, 76
- Schaye, J., Crain, R. A., Bower, R. G., et al. 2015, *MNRAS*, 446, 521
- Sheth, R. K., & Tormen, G. 1999, *MNRAS*, 308, 119
- Springel, V., Pakmor, R., Pillepich, A., et al. 2018, *MNRAS*, 475, 676
- Stefanon, M., Bouwens, R. J., Labbé, I., et al. 2021, *ApJ*, 922, 29
- Trebitsch, M., Dubois, Y., Volonteri, M., et al. 2021, *A&A*, 653, A154
- Tremmel, M., Karcher, M., Governato, F., et al. 2017, *MNRAS*, 470, 1121
- Tremmel, M., Quinn, T. R., Ricarte, A., et al. 2019, *MNRAS*, 483, 3336
- Visbal, E., Bryan, G. L., & Haiman, Z. 2020, *ApJ*, 897, 95
- Vogelsberger, M., Genel, S., Springel, V., et al. 2014a, *Natur*, 509, 177
- Vogelsberger, M., Genel, S., Springel, V., et al. 2014b, *MNRAS*, 444, 1518
- Zavala, J. A., Buat, V., Casey, C. M., et al. 2022, arXiv:2208.01816